MASTER IN MARINE SCIENCES

Option: Physical and Biogeochemical Oceanography

Aude JOËL

Characterization of oceanic fine-scale dynamics in the Western Mediterranean Sea during the BioSWOT-Med campaign

Internship realized between January and June 2024, under the supervision of: Andrea Doglioli (M.I.O), Maristella Berta (CNR-ISMAR) and Louise Rousselet (LOCEAN)

Academic Year : 2023-2024

Acknowledgments

This internship was conducted under the guidance of Andrea Doglioli (M.I.O), Maristella Berta (CNR-ISMAR), and Louise Rousselet (LOCEAN). Thanks to all of you for the opportunity to participate in the on-land adventure of BioSWOT-Med. Thank you for your time, trust, and for sharing your extensive knowledge and passion for physical oceanography throughout these intense months of work. You made this experience a great spirited one.

Special thanks to Francesco d'Ovidio (LOCEAN) for directing and supporting my work on the SWOT analysis; to Lloyd Izard (LOCEAN) for our collaboration and his lively spirit; and to Chloé Goret (LOCEAN) for our fruitful exchanges on SWOT results.

I am also grateful to the entire BioSWOT-Med community for the inspiring and continuous exchanges. In particular, thanks to the members of the physics working group; to Anne Petrenko (M.I.O), Stéphanie Barillon (M.I.O), and Maxime Arnaud (M.I.O) for their expertise on vertical velocities; to Laurina Oms (M.I.O) for sharing her latest findings with me; and to Anthony Bosse (M.I.O) and Robin Rolland (LOCEAN) for their assistance in exploring near-inertial oscillations.

Many thanks to the CNR-ISMAR team who made me feel at home in Italy, especially Annalisa Griffa for her involvement and expertise in fine-scale dynamics. I also appreciate the support from Milena Mena and Riccardo Martelucci from the National Institute of Oceanography and Experimental Geophysics (OGS), Aurélien Ponte and Margot Demol from IFREMER, and Ananda Pascual from IMEDEA (CSIC-UIB).

A special thanks to the M.I.O EcoMad team for their enthusiasm in conducting and sharing science, for the stimulating environment they cultivate, and for their feedback on my research. Last but not least, I would like to thank the M.I.O administration team, particularly Carole Mulatero and Dominique Estival, for their invaluable support.

Contents

1 Introduction

Oceanic circulation comprises multi-scale, non-linear, heterogeneous, and complex processes. Large-scale ocean circulation has been observed since the 18^{th} century, with Benjamin Franklin's description and first map of the Gulf Stream while the study of micro-scale processes dates back even further, to Leonardo da Vinci's 16^{th} century observations of turbulence. Between these scales are the mesoscale and sub-mesoscale structures, also known as fine-scale features, such as eddies, fronts, and filaments. Mesoscale eddies are characterized by a large Rossby number (the ratio of advection to Coriolis force), they can last from several days to a few months trapping water inside them. Sub-mesoscale fronts and filaments form due to flow deformation and fluid instabilities, spanning spatial range from few to tens kilometer. Fine-scale processes are ubiquitous in seas and oceans; they generate horizontal and vertical exchanges that critically affect ocean physics and ecology, extending to the climate scale. These processes are marked by intense energetic dynamics and strong gradients and play a crucial role in regulating the climate by controlling carbon, heat, and energy exchanges between the ocean and atmosphere. They favor vertical exchanges and significantly influence the stratification of the ocean's upper layer over a few days (Thomas *et al.*, 2008). Fine-scale features operate on similar time-space scales as biological processes such as phytoplankton blooms, zooplankton vertical migrations and the foraging behavior of top predators (Dickey & Bidigare, 2005; Mahadevan, 2016; McGillicuddy, 2016; Della Penna *et al.*, 2015). Oceanographic campaigns have studied the links between mesoscale and sub-mesoscale circulations (Petrenko *et al.*, 2017; Troupin *et al.*, 2019) and their interactions with biogeochemical processes (Moutin *et al.*, 2017) but, detecting and studying fine-scale structures is still challenging because they are too large for synoptic measurements by fixed Eulerian arrays of moorings, they deform too rapidly for typical *in-situ* surveys, and they were until recently too small and short-lived for satellite detection (Novelli *et al.*, 2017). These structures' fast evolution, ephemeral lifetime, and limited spatial extent have led field studies to focus on stronger and longer-lived features and a lack of empirical data on fine-scale dynamics, especially under moderate-energy circulation conditions remains.

To address it, an international scientific effort was established around the new NASA-CNES Surface Water and Ocean Topography (SWOT) satellite, launched on December 16, 2022. SWOT is equipped with cutting-edge technology, enabling two-dimensional ocean altimetry measurements instead of the traditional one-dimensional along-track measurements. This new generation of altimeter can detect circulation features as small as 7-10 km across a 150 km wide swath, which is an order of magnitude higher in resolution than current satellite altimetry capabilities. This advancement allows for the identification of upper ocean dynamics at an unprecedented resolution. Following the satellite's launch, a four-month "Fast Sampling Phase" from March to June 2023 covered specific global areas with one or two passes per day (see yellow and orange tracks on Fig.1, right). This period offered a unique opportunity for focused studies on fine-scale ocean dynamics (d'Ovidio *et al.*, 2019). The international consortium SWOT-AdAC ("Adopt a Crossover") coordinated several field campaigns to leverage this unprecedented satellite data availability. As part of the SWOT-AdAC project, the BioSWOT-Med campaign took place from April 20 to May 15, 2023, in the Western

Mediterranean Sea (Doglioli & Gregory, 2023), aboard the oceanographic vessel L'Atalante (see trajectory of the cruise on Fig.1 (left). The campaign aimed to study three main aspects of fine-scale circulation: i) the fine-scale circulation in moderate-energy and oligotrophic ocean conditions, ii) its impact on nutrient fluxes and matter export, and iii) its contribution to the high planktonic diversity. Moderate-energy and oligotrophic conditions, such as those in the Mediterranean Sea, are representative of most ocean waters and have been poorly explored compared to Western boundary currents or Eastern boundary upwellings, where the fine-scale processes are induced by strong ocean dynamics. The BioSWOT-Med campaign sampled the area northeast of Menorca (Balearic Islands), where a branch of the Northern Current (NC) operates a retroflexion eastward, forming the North Balearic Front (NBF), north-eastward to Menorca. The NBF characterizes as a seasonally and thermally driven frontal zone which acts as a hydrological and dynamical barrier between different water masses. It has a higher productivity at the north and is more oligotrophic and highly stratified at the south (Barral *et al.*, 2021). The position of the NBF varies slightly according to atmospheric forcings and is characterized by an intermittent productivity in response to the front instabilities and high variability. Previous studies have shows that this region's frontogenetic dynamics models the phytoplankton community distribution (Tzortzis *et al.*, 2021) and that the space-time variability of its fine-scale structures should be resolved by SWOT (Barceló-Llull *et al.*, 2021).

During BioSWOT-Med, an adaptive and Lagrangian strategy, was employed to target fine-scale structures in the NBF and perform numerous multi-disciplinary and multi-platforms samplings (Doglioli *et al.*, 2024). This study focuses on the data acquired from the deployment of Lagrangian drifters, designed to track currents at depths of 1-m and 15-m and equipped with GPS trackers. Through high-frequency sampling at 15-minute intervals, these drifters offer additional insights complementing the synoptic perspective provided by the SWOT satellite, facilitating the observation of ocean dynamics. Two oceanic fine-scale dynamical structures observed within a 30 km radius between May 5 and 12 will be characterized, consisting in a frontal jet and an anticyclonic eddy with a special emphasis on their interactions and how it affects the physical properties of the water masses, frontal structures being generally associated with ageostrophic vertical secondary circulation (McWilliams, 2016). Quantifying the Lagrangian properties of distinct water masses such as divergence, vorticity and strain will provide a detailed view of the fine-scale circulation present during this specific spatial and temporal window, contributing to the understanding of these complex dynamics. The estimation of vertical velocities is also relevant to meet the objectives of BioSWOT-Med since negative vertical velocities are associated with the export of organic matter and carbon (downwelling), while positive vertical velocities bring nutrients to the surface (upwelling), boosting primary production. They are yet particularly challenging to measure in oligotrophic and low energy environments such as the Mediterranean Sea: by being several orders of magnitude lower than horizontal velocities, they are hard to estimate and so far, no direct *in-situ* measurements could be performed. Their estimation remains a critical objective in physical oceanographic studies. Finally, comparing both *in-situ* and SWOT datasets will help assessing the accuracy of SWOT, with a special focus on space-time scales previously unresolved by conventional altimetry.

Table I. Summary of the drifters deployed on May 5 (in the anticyclone) and 6 (in the front) with their deployment times and locations.

DEPLOYMENT IN ANTICYCLONE – May 5th, 2023											
1m Drifters						15m drifters					
Lag. Device ID	Date	Time (UTC)	LAT	LON	Location	Lag. Device ID	Date	Time (UTC)	LAT	LON	Location
CARTHE 8923	05 May	02:44	40° 50.495'N	04° 55.605'E	ANTICY. deploy. Center	SVP-SIO 8370	05 May	03:04	40° 50.579'N	04° 56.906'E	ANTICY. deploy. 1St point
CARTHE 8926	05 May	03:20	40° 51.452'N	04° 55.444'E	ANTICY. deploy. 3Rd point	SVP-SIO 8320	05 May	03:12	40° 51.233'N	04° 56.418'E	ANTICY. deploy. 2Nd point
CARTHE 8938	05 May	03:12	40° 51.233'N	04° 56.418'E	ANTICY. deploy. 2Nd point	SVP-SIO 8910	05 May	03:20	40° 51.452'N	04° 55.444'E	ANTICY. deploy. 3Rd point
CARTHE 8942	05 May	03:53	40° 49.490'N	04° 55.919'E	ANTICY. deploy. 7Th point	SVP-SIO 5970	05 May	03:28	40° 51.042'N	04° 54.533'E	ANTICY. deploy. 4Th point
CARTHE 8943	05 May	04:01	40° 49.956'N	04° 56.348'E	ANTICY. deploy. 8Th point	SVP-SIO 0460	05 May	03:37	40° 50.266'N	04° 54.318'E	ANTICY. deploy. 5Thpoint
CARTHE 9009	05 May	03:04	40° 50.579'N	04° 56.906'E	ANTICY. deploy. 1St point	SVP-SIO 5960	05 May	03:45	40° 49.627'N	04° 54.908'E	ANTICY. deploy. 6Th point
CARTHE 9089	05 May	03:45	40° 49.627'N	04° 54.908'E	ANTICY. deploy. 6Th point	SVP-SIO 0510	05 May	03:53	40° 49.490'N	04° 55.919'E	ANTICY. deploy. 7Th point
CARTHE 9458	05 May	03:37	40° 50.266'N	04° 54.318'E	ANTICY. deploy. 5Th point	SVP-SIO 5980	05 May	04:01	40° 49.956'N	04° 56.348'E	ANTICY. deploy. 8St point
CARTHE 9467	05 May	03:28	40° 51.042'N	04° 54.533'E	ANTICY. deploy. 4Th point	BGC-SVP	05 May	02:44	40° 50.495'N	04° 55.605'E	ANTICY. deploy. Center
DEPLOYMENT IN FRONT – May 6th, 2023											
1m Drifters						15m drifters					
Lag. Device ID	Date	Time (UTC)	LAT	LON	Location	Lag. Device ID	Date	Time (UTC)	LAT	LON	Location
CODE 65	06 May	13:32	41° 12.086'N	05° 08.971'E	FRONT deploy. 2Nd point	SVP-OGS 3890	06 May	13:15	41° 13.641'N	05° 08.304'E	FRONT deploy. 1St point
CODE 64	06 May	12:35	41° 12.003'N	05° 05.011'E	FRONT deploy. Center	SVP-OGS 3920	06 May	12:35	41° 12.003'N	05° 05.011'E	FRONT deploy. Center
CODE 66	06 May	13:47	41° 10.679'N	05° 08.558'E	FRONT deploy. 3Rd point	SVP-OGS 4890	06 May	14:03	41° 09.458'N	05° 07.080'E	FRONT deploy. 4Th point
CODE 67	06 May	14:19	41° 09.005'N	05° 05.080'E	FRONT deploy. 5Th point	SVP-OGS 4920	06 May	14:51	41° 10.487'N	05° 01.574'E	FRONT deploy. 7Th pointr
CODE 68	06 May	14:35	41° 09.376'N	05° 03.093'E	FRONT deploy. 6Th point	SVP-OGS 6800	06 May	15:39	41° 14.640'N	05° 03.061'E	FRONT deploy. 10Th point
CODE 69	06 May	15:07	41° 11.989'N	05° 01.024'E	FRONT deploy. 8Th point						
CODE 70	06 May	15:23	41° 13.517'N	05° 01.545'E	FRONT deploy. 9Th point						
CODE 71	06 May	15:55	41° 15.012'N	05° 05.097'E	FRONT deploy. 11Th point						
CODE 72	06 May	16:10	41° 14.606'N	05° 07.017'E	FRONT deploy. 12Th point						

2 Materials and methods

2.1 Adaptive and Lagrangian sampling strategies

The precise selection of the sampling zone was based on an **adaptive sampling strategy** using the SPASSO software (Software Package for Adaptive Satellite-based Sampling for Oceanographic Cruises, available at https://spasso.mio.osupytheas.fr/) (Rousselet *et al.*, submitted), which has been upgraded within the SWOT-AdAC consortium. Using several datasets from the CMEMS (Copernicus Marine Environment Monitoring Service), Nasa and CLS (Collecte Satellite Toulouse), SPASSO provides daily reports on sea-surface height (ssh) and derived currents, sea-surface temperatures, and surface chlorophyll-a concentrations in the cruise area, as well as maps of Lagrangian-derived diagnostics allowing for the identification of fine-scale features. The zone was monitored from space for several weeks before departure and continually monitored during the cruise in order to target suitable fine-scale structures and plan the route. SPASSO identified a region 100 km northeast of Menorca with markedly contrasting chlorophyll concentrations, indicative of a front. Initial SWOT images received from CNES (Centre National d'études spatiales) on April 6 also suggested the presence of a front and an anticyclonic eddy, providing ideal conditions for studying fine-scale dynamics. A **Lagrangian sampling strategy** was implemented to gather physical and biogeochemical samples, incorporating sampling transects and drifting stations. This study focuses on two intensive and targeted drifter deployments on May 5 and 6, within the anticyclonic and frontal features respectively.

2.2 *In-situ* Lagrangian measurements

2.2.1 Drifting buoys and surface currents

During the BioSWOT-Med campaign, two primary types of drifters were deployed. The first type comprises drifters designed to track currents within a depth of 1 meter, known as CARTHE (Consortium of Advanced Research on the Transport of Hydrocarbons in the Environment) (Novelli *et al.*,

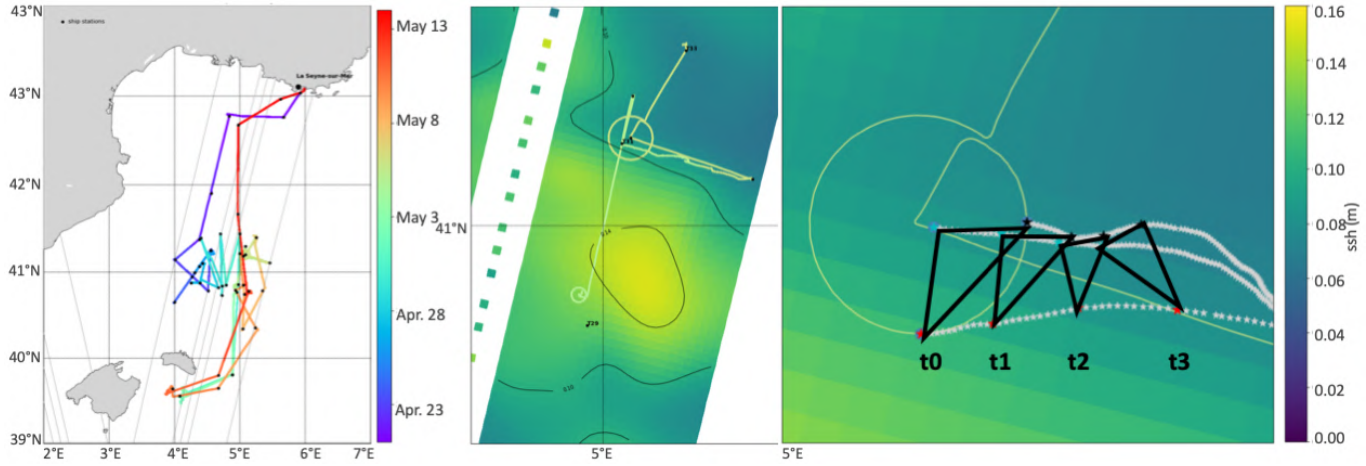

Figure 1. Left: trajectory of the BioSWOT-Med campaign from April 20 to May 15 2023. Middle: zoom-in on the ship trajectory on May 5 and 6. The circle located at the south (north) locate the position of the drifters deployed in the anticyclone (front) on May 5 (6) superimposed on SWOT ssh (m) of May 6. Right: example of trajectories of a triplet of drifters (in grey) and evolution of its 2-D geometrical shape, size and orientation (in black) over time.

2017) and CODE (Coastal Ocean Dynamics Experiment) (Davis, 1985). The second type includes SVPs (Surface Velocity Program) (Niiler *et al.*, 1995) designed to monitor currents at a depth of 15 meters. All drifters were configured to transmit their latitude and longitude coordinates every 15 minutes. On May 5, nine CARTHE drifters and nine SVPs were deployed in an anticyclonic feature. On May 6, nine CODE drifters and five SVPs were deployed in a frontal feature (their deployment locations and times are detailed in Table I). Additionally, two ARGO float platforms, deployed on April 28 and May 5, will be analysed in this study. They were programmed with a 6-hour cycling period to obtain high resolution samplings. Their parking depth was disregarded and the imposed cycle allowed the float to reach a maximum depth between 300 and 400 meters before surfacing and transmitting their positions and water column biophysical properties. Three other SVPs deployed during the C-SWOT campaign (Garreau, 2023) organized from May 28 to April 18, 2023, will be considered in this study as well.

2.2.2 Strategy of deployment and Lagrangian properties

Following the drifters trajectories allows for assessing the kinematic properties (KP) of the water masses sampled, in particular the **divergence** (D), which indicates whether fluid parcels are converging or diverging, the **vorticity** (ζ) which provides insights into the rotational tendencies of particles and the normal and shear **strain** (N_{st} and S_{st}) representing the deformation of the fluid, characterized by stretching and shearing. These properties can be estimated using eq.(1) to (5), where u and v (in m s^{-1}) denote the horizontal velocities along the east-west and north-south axes.

$$D = \frac{\partial u}{\partial x} + \frac{\partial v}{\partial y} \rightarrow \frac{1}{A}\frac{dA}{dt} \tag{1}$$

$$\zeta = \frac{\partial v}{\partial x} - \frac{\partial u}{\partial y} = \frac{\partial u'}{\partial x} + \frac{\partial v'}{\partial y} \rightarrow \frac{1}{A'}\frac{dA'}{dt} \tag{2}$$

$$N_{st} = \frac{\partial u}{\partial x} - \frac{\partial v}{\partial y} = \frac{\partial u"}{\partial x} + \frac{\partial v"}{\partial y} \rightarrow \frac{1}{A"}\frac{dA"}{dt} \tag{3}$$

$$S_{st} = \frac{\partial v}{\partial x} + \frac{\partial u}{\partial y} = \frac{\partial u"'}{\partial x} + \frac{\partial v"'}{\partial y} \rightarrow \frac{1}{A"'}\frac{dA"'}{dt} \tag{4}$$

$$Strain = \sqrt{N_{st}^2 + S_{st}^2} \tag{5}$$

These equations are based on the **area rate of change method**. Initially established in atmospheric studies (Saucier, 1953) and later generalized to oceanography (Molinari & Kirwan, 1975), this method uses the successive positions of the drifters identified as sets of "triplets" forming triangular shapes on an horizontal area A. The specific deployment on a circle ensures the maximization of triplet combinations: Fig.1 shows the ship's trajectory (left) over the entire cruise period and a zoom-in over May 5 and 6 (middle) with the two circles designed to sample the anticyclonic (south) and frontal (north) features. The drifters were deployed over a period of a few hours on those circles a few kilometers-wide compatible in size with the targeted fine-scale structures, with an additional drifter placed at the circle's center. At each time step (here 15 minutes), the triangular portion of surface water enclosed within each triplet undergoes changes in size, shape, and orientation as the drifters disperse due to ocean currents. The evolution of the 2-D geometric shape of each triplet is expressed as the fractional time rate of change of the area A. If A increases (decreases) over time, it means that the drifters are moving apart (getting closer), resulting in a positive divergence (negative convergence) (eq.1). By applying a 90° clockwise rotation to the u and v components (where u becomes -v and v becomes u), a new area A' is defined, providing an estimation of the vorticity (eq.2). Positive (negative) vorticity corresponds to a cyclonic (anticyclonic) circulation in the northern hemisphere. Further transformations of the u and v components are applied to obtain N_{st} with $A"$ (where u remains u and v becomes -v) (eq.3), and S_{st} with $A"'$ (where u becomes v and v becomes u) (eq.4). When combined, eq.3 and eq.4 provide the strain (eq.5), characterizing the deformation of the fluid, with values close to 0 indicating no strain and values on the order of f (or higher) indicating significant deformation. In this study, KPs are estimated at both 1-m and 15-m depths and normalized by the local Coriolis parameter f (see 2.2.3), which allows for the determination of the prevailing processes. KPs much smaller than f indicate geostrophic mesoscale activity, while values comparable or higher than f indicate ageostrophic sub-mesoscale activity.

In this method, size range for triplet selection is critical according to the desired targeted feature: a range too small does not provide enough triplets for the analysis over time, while a range too large may combine drifters from different fine-scale structures, making them unsuitable for a Lagrangian analysis. In this study, the chosen range was set from 0.2 to 15 km based on sensitivity tests. The lower bound was based on the nominal uncertainty in the GPS drifter position (of order of tens of meters), while the upper bound is chosen to encompass the fine-scale anticyclonic and frontal features targeted (less than a third of the scale of the targeted features). The estimation of KPs is feasible

as long as the drifters forming the triplets maintain a non-collinear configuration. An aspect ratio (AR) of the 2-D geometrical form is defined as in eq.6, varying from 0 (a flat line) to 1 (a perfect equilateral triangle), with P the perimeter formed by each triplet.

$$AR = \sqrt{2 * 6^3}\frac{A}{P^2}; \tag{6}$$

Only triplets with an AR > 0.2 are considered (Esposito *et al.*, 2021; Huntley *et al.*, 2019). The availability of the divergence property estimates at both 1-m and 15-m depths offers the opportunity to estimate vertical velocities within the surface layer. This is achieved by integrating the Equation of Continuity (based on the assumption of the fluid incompressibility) between 1-m and 15-m depths, with the divergence defined as $\mathrm{D} = -\frac{\partial w}{\partial z}$, where w represents the vertical velocity in m s^{-1}. Estimating w requires coincident values of divergence in space and time at the two depths so, for each depth, the divergence values are binned and averaged over a day on a grid of 1km by 1km and D is expressed as the mean value of the divergence at 1 m and 15m in each bin. This yields an estimation of vertical velocities over a 15-meter depth interval, usually expressed in meters per day, with positive (negative) values indicates upwelling (downwelling) motions.

2.2.3 Drifter dataset cleaning

As the initial step of this study, all raw datasets from the drifters underwent a thorough cleaning process. This involved the removal of data recorded before deployment (during drifter testing) and, when applicable, after retrieval or grounding on the coast. Consecutive repeated data points in drifter trajectories with identical latitude/longitude pairs or timestamps were eliminated, along with outlier values identified through an acceleration-based filter. This preparatory work laid the ground for the so-called Level 1 treatment, which will be standard practice for processing SWOT-AdAC campaigns drifter datasets. Trajectories were then interpolated to generate a uniformly sampled dataset with a 15-minute interval, necessary step to conduct Lagrangian diagnostics. Notably, near-inertial oscillations (NIOs) were observed in the trajectories. To facilitate comparison with SWOT data, a 4^{th} order Butterworth low-pass filter, with a cut-off period of 24 hours, was applied to remove these oscillations. The theoretical inertial period is defined as $\mathrm{T} = \frac{2*\pi}{f}$ (in s), where f represents the Coriolis parameter with $\mathrm{f} = 2.\Omega.\sin(\Phi)$ in s^{-1}, and with Ω the Earth angular velocity with $\Omega = 7.2921\ 10^{-5}$ in rad s^{-1}. In this study, f was calculated at a mean latitude of 41°N ($f = 9.3954\ 10^{-5}$ s^{-1}) resulting in an inertial period T of approximately 18.6 hours.

2.3 Remote sensing measurements

2.3.1 Principles of satellite altimetry

Altimetry measures the distance between the satellite orbit and the ocean surface (R) by emitting electromagnetic waves towards the Earth's surface and calculating their return time. It also determines its distance to the reference ellipsoid (H), which approximates the geoid, an equipotential reference surface for the Earth's gravity field. The sea-surface height (ssh) is then defined by

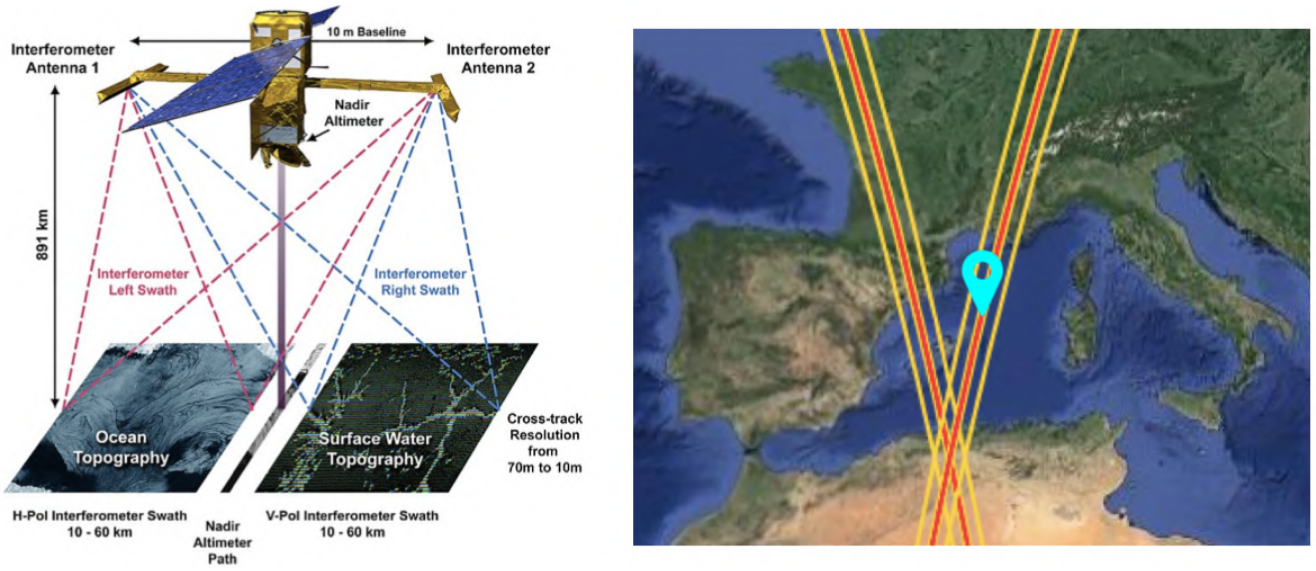

Figure 2. Left: representation of SWOT satellite and its system of measurements (source: NASA). Right: location of SWOT swaths (yellow and orange) during the fast-sampling phase and location of BioSWOT-Med campaign (blue icon) (source: https://www.swot-adac.org/)

the equation η = H - R. Using the geostrophic and hydrostatic approximations, the Navier-Stokes equations yield the altimetry-derived geostrophic velocities (in m s^{-1}):

$$u = -\frac{g}{f} \cdot \frac{\partial \eta}{\partial y} \qquad\qquad v = \frac{g}{f} \cdot \frac{\partial \eta}{\partial x} \tag{7}$$

Classical altimetry satellites measure ssh at the nadir along the orbit-track which is a few kilometers wide only. The data are then corrected and interpolated in both space and time to provide a synoptic view of ssh. This study use the CMEMS multi-satellite product DUACS (Data Unification and Altimeter Combination System, doi: 10.48670/moi-00142) which integrates data from multiple satellites, including TOPEX/POSEIDON, GFO, and JASON. The Mediterranean Sea product has a ground resolution of 1/8 degree, allowing the identification of dynamical features as small as 75-100 km.

2.3.2 SWOT satellite

In addition to a classical nadir altimeter like the previous generations of satellites, the new SWOT satellite also features a KaRIn (Ka-band Radar Interferometer) imaging radar, which operates with two radar antennas located at the ends of 10-meter masts (Fig.2, left). Consequently, it also provides ssh data (and derived geostrophic velocities) in two 50 km-wide swaths separated by a 20 km gap, with a 2 km grid resolution. This enables the detection of fine-scale structures down to 7-10 km. Compared to conventional altimetry, SWOT also offers a better resolution near the coasts. An example of the difference in spatial resolution between SWOT and previous generations of altimetry satellites is shown in Fig.3 with ssh (left) and velocities (right) in the daily ground track of SWOT during the four-months calibration and validation phase in the region of the BioSWOT-Med cruise. The SWOT data used in this study were released in September 2023 (v0.3, L3 treatment including ssh, u, and v). SWOT's enhanced capabilities allow for the identification of oceanic fine-scale circulation

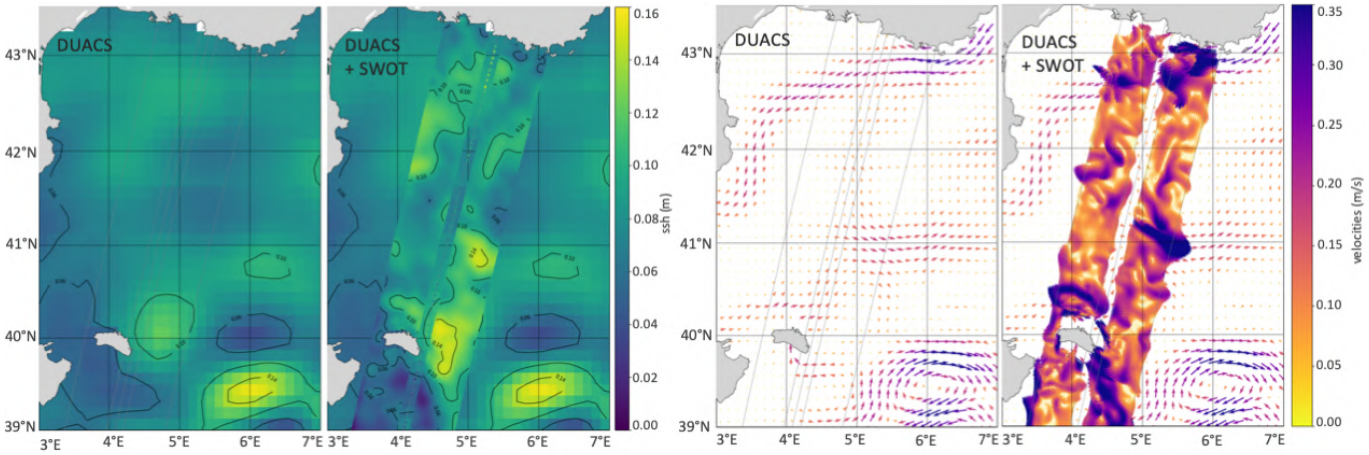

Figure 3. Vizualisation of ssh (m) (left) and geostrophic velocities (right) from DUACS and from SWOT superimposed on DUACS, on May 8, 2023.

features, such as eddies and fronts, and the differentiation between eddy cores and their peripheries which opens a new field of investigation into fine-scale ocean circulation.

2.3.3 LAMTA toolbox for Lagrangian diagnostics

The LAgrangian Manifolds and Trajectories Analyser (LAMTA) (d'Ovidio *et al.*, 2015; Rousselet *et al.*, submitted) is a set of functions designed to perform Lagrangian analysis using oceanic 2-D velocity fields. The routines can simulate numerical particle trajectories both backward and forward using a Runge–Kutta fourth-order advection scheme, and can also compute Lagrangian diagnostics. In this study, the LAMTA package was utilized to simulate the drifters' trajectories using both DUACS and SWOT velocities for comparison and better assess the local ocean circulation.

2.3.4 Complementary satellite products

Other CMEMS products were used in this study to provide additional information. Daily maps of chlorophyll *a* were extracted from the "Sentinel-3 OLCI L1B" satellite product (doi: 10.48670/moi-00295). Hourly wind velocity fields were extracted from the "Global Ocean Hourly Sea Surface Wind and Stress from Scatterometer and Model" product (doi: 10.48670/moi-00305), which combines satellite observations and modeling. Mean estimation over 6h and 24h were used for the analysis.

3 Results

3.1 Drifters' trajectories and identification of fine-scale structures

The drifter trajectories of are shown on Fig.4: on the top are the CARTHE and CODE drifters (left) and SVP drifters (right) from the day of their deployment, on May 5 and 6, until May 12. After that date, the drifters were too dispersed, out of the 0.2-15 km range, to estimate kinematic properties (KPs) using the area rate of change method. The 1-m drifters deployed in the targeted eddy followed an anticyclonic circulation pattern with near-inertial oscillations (NIOs) until the end of May

8, before deviating southward. In contrast, the 15-m drifters remained in the anticyclonic feature for the entire study period. It took them 4 days to do a full loop in the eddy. The 1-m drifters traced a wider circle than the 15-m drifters, suggesting a conical eddy structure. The trajectories also indicate that the eddy has an elliptical shape, stretched along a NE-SW axis. Notably, the SVPs drifters remained trapped in the eddy for several days, leaving the eddy between on the 14^{th} and the 19^{th}, with a decreasing radius over time. The drifters deployed on May 6 in the targeted frontal feature were quickly carried away in a southeast direction, exhibiting no inertial oscillations during the first days (until the end of May 7). As for the anticyclonic drifters, at the end of May 8, their trajectories shifted toward a northeast direction, with the emergence of a NIOs signature that persisted until the end of the study period. This initial analysis suggests that SWOT images provided in near real time during the cruise successfully identified different coexisting fine-scale structures within a 30 km wide area.

This analysis is strengthened by additional trajectories from two ARGO float profilers: the first captured at the edge of the anticyclonic eddy and the second looped in its center (Fig.4, bottom left), confirming the persistence of the eddy down to a depth of at least 300m. Additionally, three SVPs deployed during the previous cruise C-SWOT drifted in the transition area between the eddy and the front during the same period (bottom right). Two of these SVPs exited the eddy, while the third one remained trapped. It took about seven days for the ARGO float at the edge of the eddy and the C-SWOT SVP that stayed in the anticyclone to complete a full loop. This also suggests that both the BioSWOT-Med 1-m and 15-m drifters were deployed within the solid-body rotation of the anticyclone, and that an external event caused the 1-m drifters to exit the eddy on May 8.

3.2 Quantification of physical processes: Lagrangian diagnostics

As shown in Fig.5 (left), in the anticyclone, the divergence/f diagnostics at both 1-m (top) and 15-m (bottom) depths exhibit a mixed signal, with positive (in red) and negative (in blue) values alternating between f and -f along the drifter' trajectories. In the frontal area, negative divergence/f predominates at the beginning of the trajectories at 1-m but rapidly get mixed. At 15-m, less divergence/f values were computed due to a significant velocity shear in the frontal zone causing the triplet sizes to exceed the defined 15 km range interval and an aspect ratio < 0.2, as suggested by the high values of strain observed (see below). After May 8, at both depths and in both features, estimates become less contrasted with values closer to zero.

The vorticity/f diagnostics (Fig.5, middle) at 1-m depth exhibits a significant shift in both structures around May 8. In the anticyclone, vorticity is initially negative, varying mostly from -0.5f to -f (in blue), indicating a consistent anticyclonic circulation on the first 3 days after the drifter deployment. Vorticity turns positive (in red) on May 8, with values mainly below 0.5f and peaks higher than 0.75-1f, indicating a cyclonic circulation as the trajectories deviate southward out of the main eddy pattern. Conversely, in the frontal structure, vorticity/f is initially positive until May 8, in the order of f and higher, when trajectories change direction and become negative, mostly in

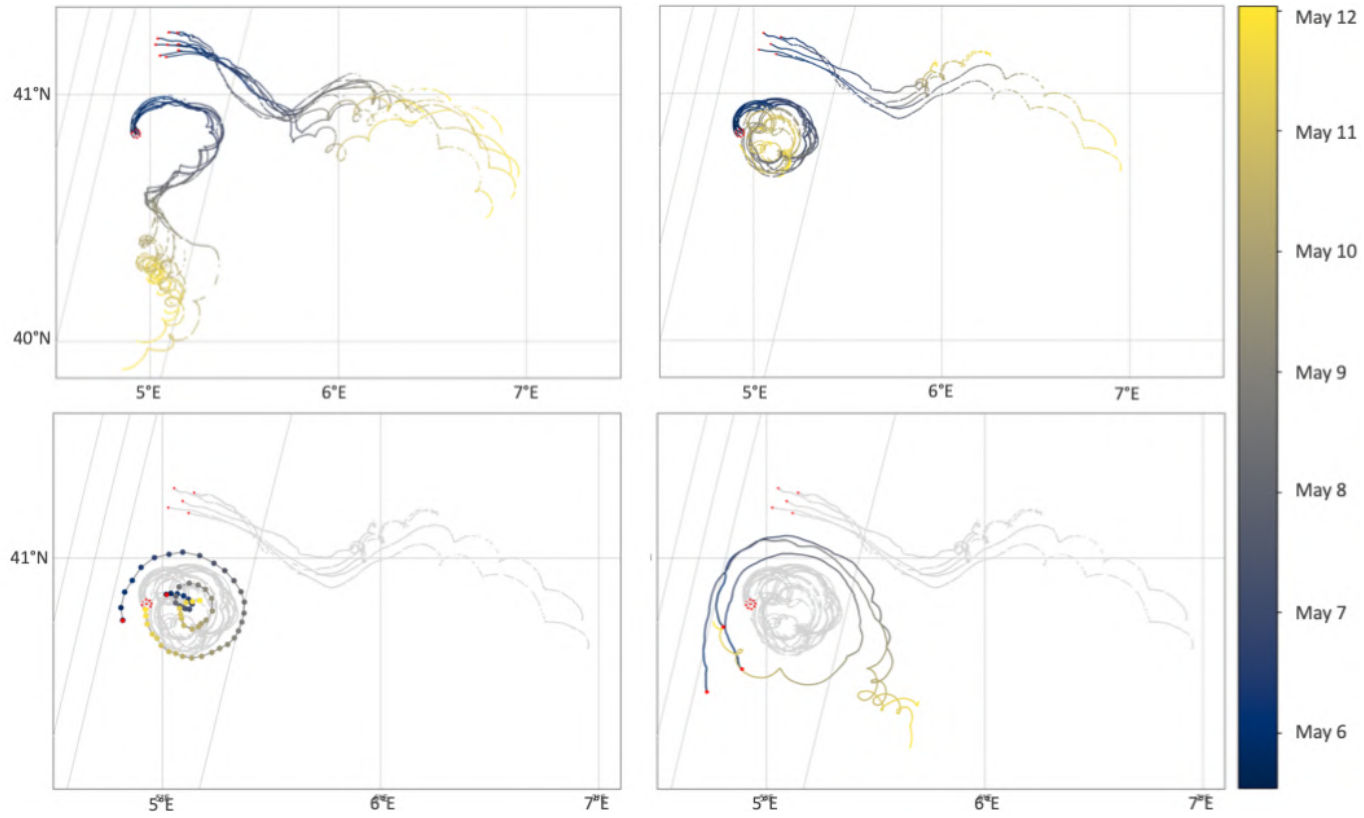

Figure 4. Top: trajectories of 1-m (left) and 15-m drifters (right) launched on May 5 in the eddy, and on May 6 in the front. Bottom: superposition of the trajectories of two ARGO floats (reaching depths until 300-400m) (left) and three SVPs (15 m) from the C-SWOT campaign (right) from May 5 to 12. They are plotted over the BioSWOT-Med SVPs trajectories (light grey). Red points indicates the deployment position of the BioSWOT-Med drifters and the positions of the ARGO-floats and C-SWOT SVPs on May 5.

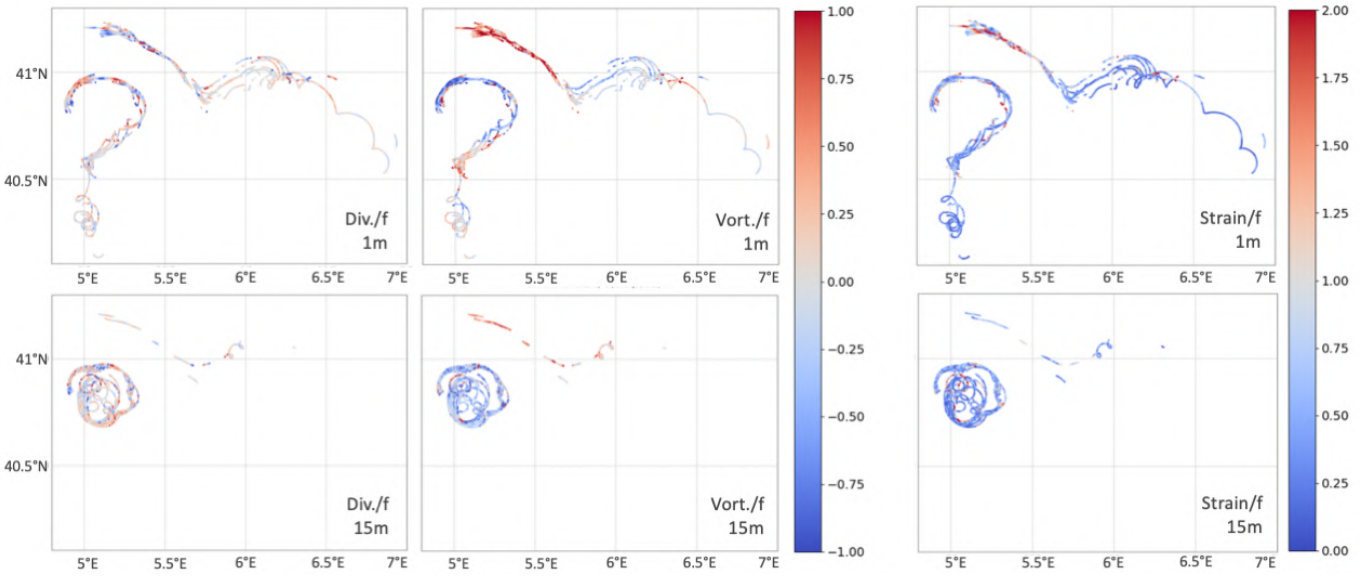

Figure 5. Lagrangian properties of the water masses estimated with drifters' trajectories from May 5 to 12: divergence D/f (left),vorticity ζ/f (middle) and strain/f (right), at 1 m (top) and at 15 m (bottom).

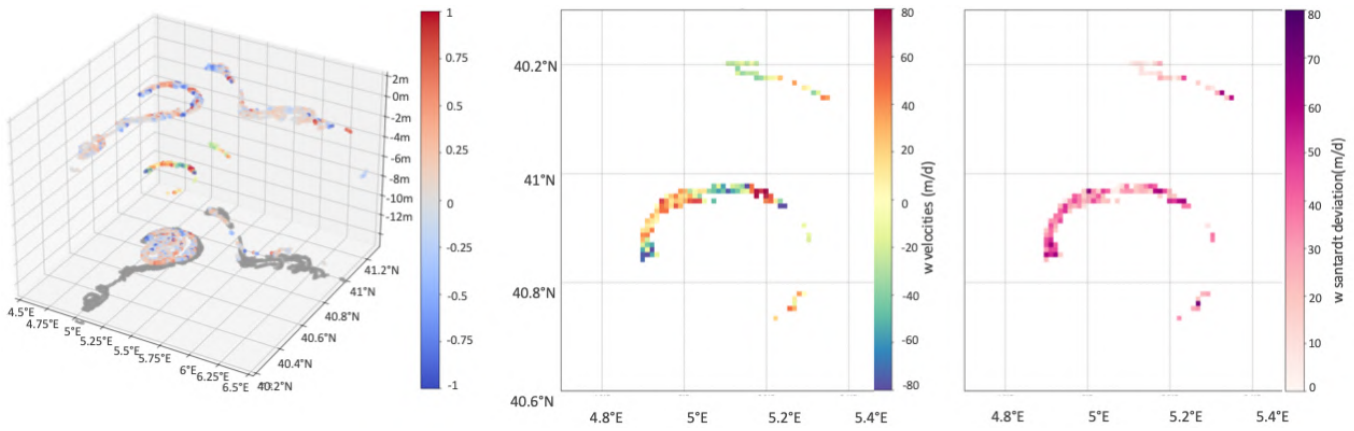

Figure 6. Estimation of vertical velocities w (m d^{-1}). Left: divergence/f at 1-m and 15-m in 3-D with w estimates in between, on a 1 km by 1km grid resolution. w values are available only where divergence/f values superimpose at both depths. Middle: w values in 2-D plot. Right: w standard deviation.

between 0 and -0.5f. This pattern is not observed at a 15-m depth, where vorticity is predominantly negative (close to -f) in the anticyclone and positive (close to f) in the frontal area all along.

The strain Lagrangian diagnostics (Fig.5, right) reveals a weak signal mainly below f (in dark blue), indicating a minimal deformation along almost every part of the drifters' trajectories, both at 1-m and 15-m depths. The only exception is observed at the beginning of the frontal structure at 1-m depth, where a peak reaching 2f at the sea surface in the western part of the front indicates significant deformation. Especially within the eddy, the vorticity magnitude prevails over the strain signal, confirming that drifters were trapped in a coherent eddy structure whereas in the surface layer of the western part of the front, the strain magnitude prevails over the vorticity signal, confirming the presence of an interface area between contrasting water masses.

Vertical velocity w estimations are possible in both the eddy and frontal structures when divergence values are collocated in the same vertical axis at 1-m and 15-m, until the drifters' trajectories began to split away two days after the deployment (Fig.6, left). The 2-D representation of w (middle) reveals an alternating pattern of negative (blue) and positive (red) values in the anticyclone, consistent with the alternating divergence pattern observed at both 1-m and 15-m depths. Extreme values of w reach up from -103 to +85 m d^{-1}. In the frontal region, w values are initially slightly negative before becoming positive. This range of vertical velocities is consistent with those found in the Alboran Sea (between +/-100 m d^{-1}) using a similar method in a frontal feature (Tarry *et al.*, 2021, 2022, Esposito *et al.*, 2023). The standard deviation of w (right) is substantial, mostly around 30 m d^{-1} (up to 50 m d^{-1}), reflecting the high variability of the local fine-scale circulation.

3.3 SWOT derived-current assessment

The comparison between drifter trajectories and SWOT data can offer valuable insights into the local surface oceanic circulation. However, before conducting such an analysis, it is essential to assess the

accuracy of the SWOT data. Interestingly, drifters in the anticyclone, both at 1-m and 15-m depths, remained within the right SWOT swath from May 5 to 12. This presents an opportunity to evaluate how some of the kinematic properties derived from satellite altimetry compare to those observed in the drifters' trajectories.

For this purpose, a low-pass Butterworth filter was applied to remove the NIOs present in the drifter trajectories, as SWOT is unable to detect such phenomena signals (see filtered trajectories on Fig.7, top). The rotary spectrum (Fig.7, bottom), derived from a Fourier analysis of the periodic signals within the trajectories, was utilized to identify different frequency components before and after filtering. It illustrates the amplitude distribution of various frequencies in the signal for unfiltered (dotted line) and filtered trajectories (solid line) of both 1-m (left) and 15-m (right) depth drifters. The representation decomposes the clockwise signal (anticyclonic, in grey) and counter-clockwise (cyclonic, in black). In both depth scenarios, the unfiltered trajectories exhibit a peak in the clockwise signal at frequencies of $1.45.10^{-5}$ and $1.32.10^{-5}$ s^{-1}, corresponding to periods of 19.1 and 21.0 h respectively, indicating the presence of NIOs (slightly higher than the theoretical 18.6-hour period at that latitude). These peaks disappear from the filtered trajectories, suggesting effective removal of the observed NIOs by the Butterworth filter. Moreover, both the unfiltered and filtered trajectories spectra of clockwise motion display another peak at a frequency of $2.95.10^{-6}$ s^{-1}, which corresponds to a period of 3.9 days. This observation is consistent with the period over which the SVPs drifters in the anticyclone eddy completed one rotation.

To facilitate the comparison between drifter and satellite altimetry data, a bi-linear interpolation was employed to more accurately approximate the 2-D SWOT velocity u and v values at the positions of the drifters. Fig.8 compares the u and v velocities recorded by the drifters (y-axis) with those derived from DUACS (first column) and SWOT (second column) altimetry observations (x-axis). The first row presents results for drifters deployed in the anticyclone, while the second row depicts those in the frontal region. The visual comparison clearly indicates that SWOT data exhibit a closer match to the drifters' data compared to DUACS. A linear regression was employed to refine the analysis. The correlation coefficient r, which measures the association between drifter and satellite velocity values, is respectively for the anticyclone and frontal areas 0.35 and 0.93 for DUACS and 0.65 and 0.98 for SWOT, indicating a stronger relationship between the measures using SWOT data. r values in the anticyclone are equal to 0.62 and 0.67 at 1 m and 15 m respectively, and equal to 0.98 in the front at both depths indicating that DUACS and SWOT have a better ability to measure currents in the frontal zone rather than in the eddy feature. To go further in the comparison of DUACS and SWOT, the computation of the regression model gives more information: the p-value for both is extremely close to 0 ($<$ 2.2e-16) indicating that they are both significant. The residual standard error (RSE) of 0.15 and 0.12 for the comparison with DUACS and SWOT dataset respectively and the R^2 (which represent the proportion of variation in the model that can be explained by the model) is of 0.12 and 0.41 for DUACS and SWOT respectively. A lower RSE and a higher R^2 also indicates that SWOT data better match the data given by the drifter trajectories.

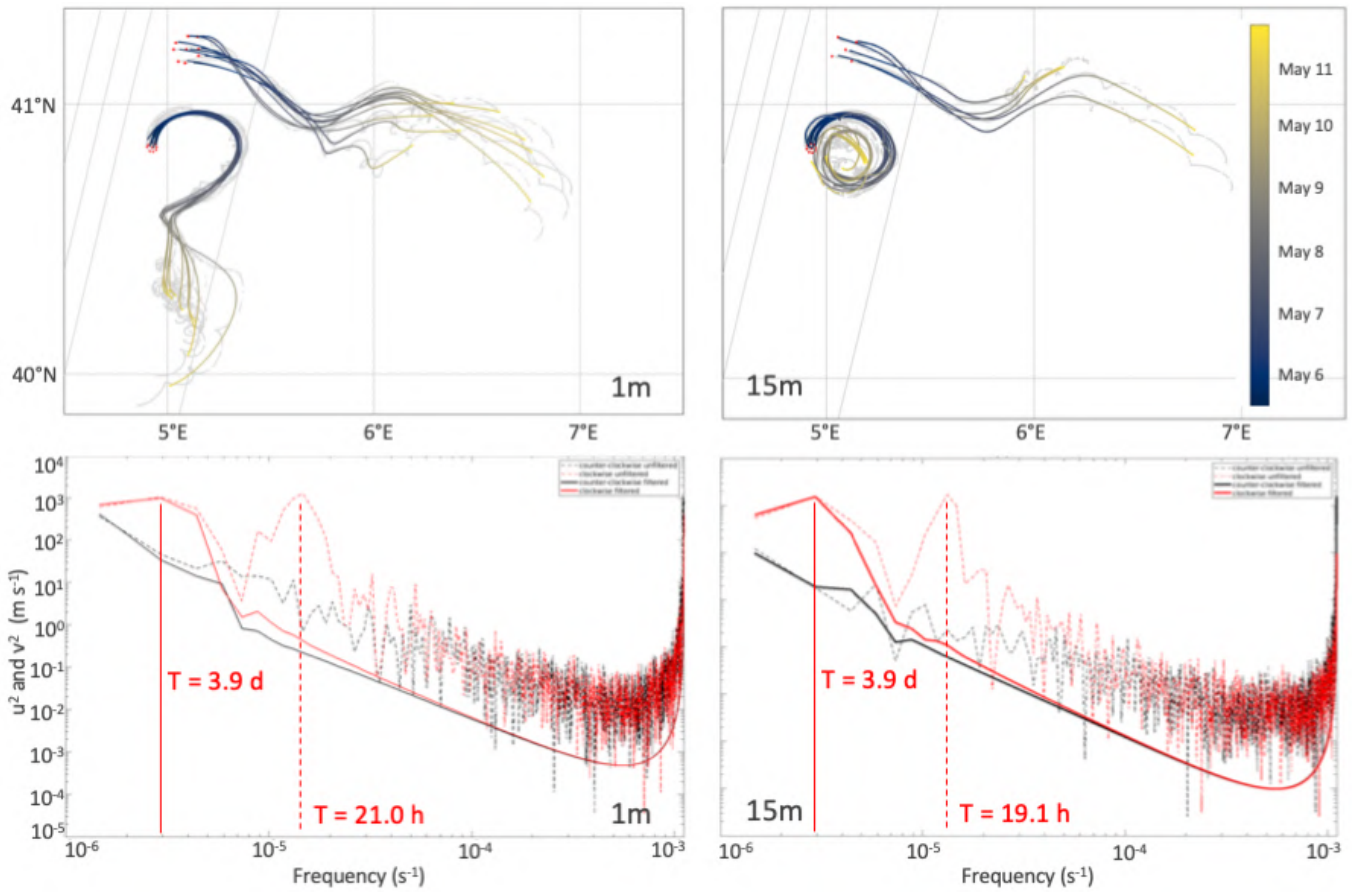

Figure 7. Top: unfiltered (in grey) and filtered (in color) drifters trajectories from May 5 to 12 at 1 m (left) and 15 m (right). Bottom: rotary spectra of their associated velocities. Dotted and solid lines show respectively signals before and after filtering the trajectories. In red are the counter-clockwise signal and in black the clockwise one.

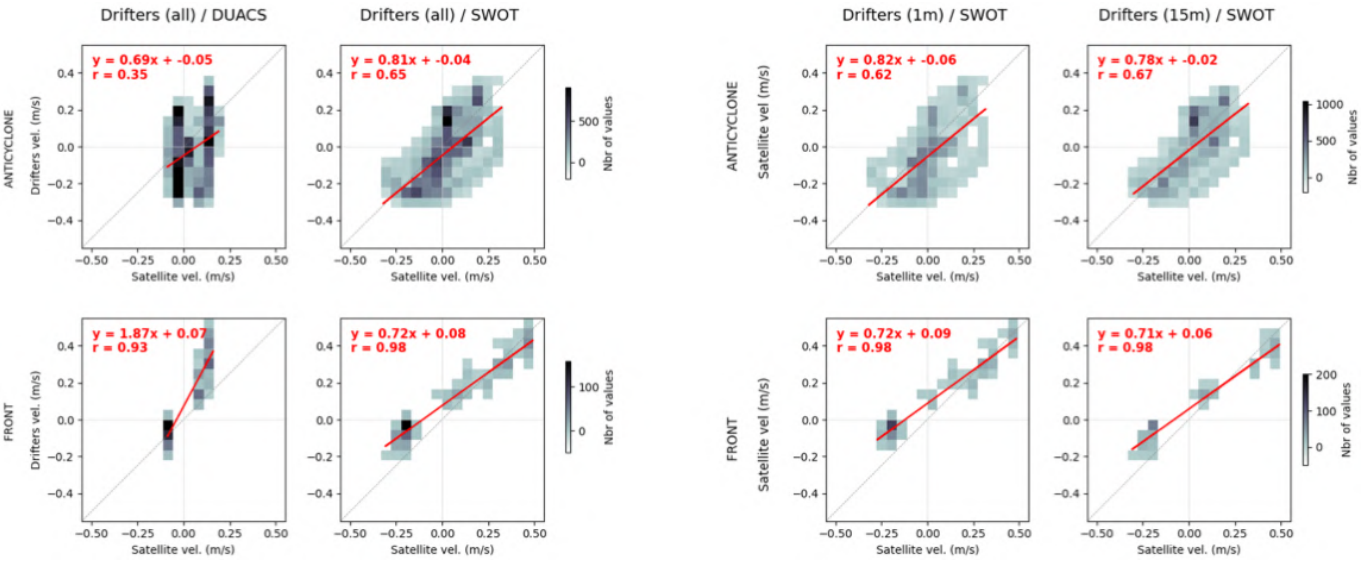

Figure 8. Density plots comparing the u and v velocities (in m s^{-1}) of the drifters (on the y-axis) and of the satellites (on the x-axis): DUACS (first column) and SWOT (second column). SWOT data compared to drifter data are also differentiated according to 1-m drifters (third column) and 15-m drifters (fourth column). The first row presents the data collected in the anticyclonic feature and the the second row in the front. The linear regressions are represented in red.

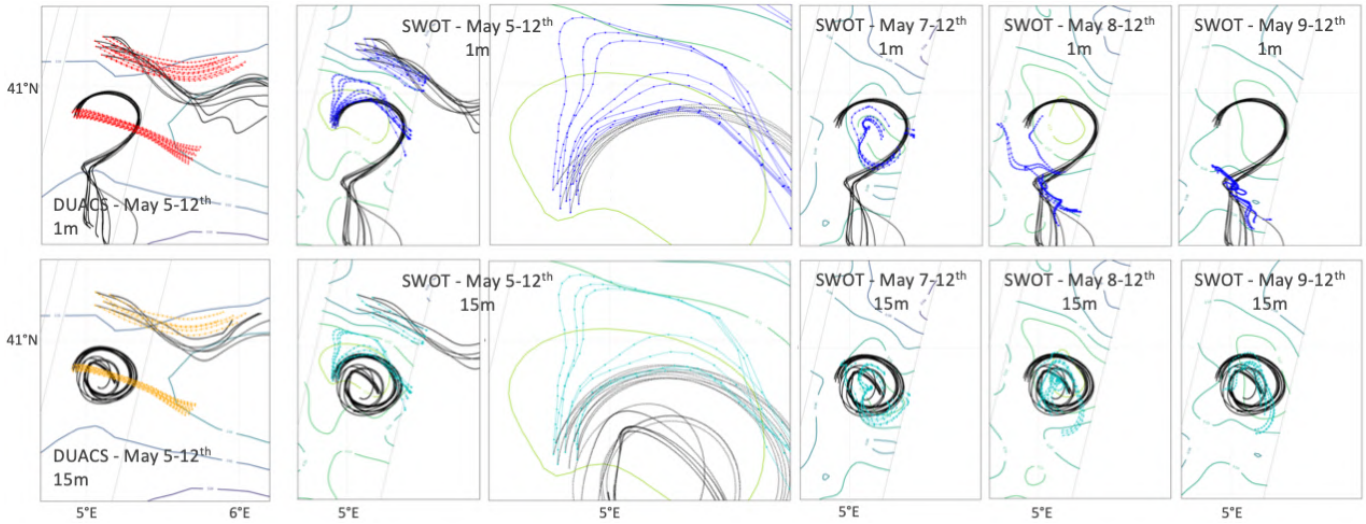

Figure 9. Simulation of numerical 1-m drifters (in red/blue on the first row) and 15-m drifters (in orange/cyan on the second row) drifters made with the LAMTA toolbox with velocities fields from DUACS (first column) and SWOT (second column) over the period May 5 to 12 with a zoom on the trajectories right after being initialized (third column). In black are the filtered drifter trajectories from May 5 to 12. The fourth, fifth and sixth columns simulate numerical particles initialized with the drifters' positions respectively on the 7 at 12am, the 8 at 12am and the 9 at 12am.

The LAMTA toolbox was utilized to simulate the advection of numerical particles initialized with the positions and times of the drifters deployment. Fig.9 compares numerical particles advected from May 5 to May 12 using DUACS velocity fields (first column in red and orange) and SWOT velocity fields (second column in blue and cyan). They are compared with the drifter trajectories at 1-m (on the top) and 15-m (on the bottom) depths in black. In the anticyclone, numerical particles simulated with DUACS exhibit strong and continuous advection toward the East, indicating a failure to identify the fine-scale structure, unlike SWOT, which shows trajectories more closely aligned with the drifter's ones. A zoom on the deployment area (third column) reveals that for numerical particles initialized at only a few kilometers of distance, trajectories exhibit varying behaviors compared to the 1-m (in blue, at the top) drifter trajectories and the 15-m (in cyan, at the bottom) drifter trajectories: some of the 1-m particles reasonably follow the drifter trajectories in the initial days, while others are deviated north before turning east and eventually converging with the black drifter trajectories, albeit with a time lag. At both depths, the particles are eventually ejected from the SWOT swath before the end of the simulation time, as the eastern part of the eddy lies at the edge of the swath. Regarding the particles initialized in the front on May 6 (second column), all of them exit the SWOT swath after one day of simulation, which is insufficient to obtain adequate information on their numerical trajectories. Additional simulations were conducted by initializing numerical particles with the drifters' positions on May 7 at 12:00 (fourth column), May 8 at 12:00 (fifth column), and May 9 at 12:00 (last column), corresponding respectively to periods before, during, and after a wind event that occurred on May 8, further investigated in Section 4.2. When particles are initialized on May 7 at 12:00, some of the 1-m particles still exit the swath, but others remain within it and continue looping in the eddy, deviating from the drifter trajectories. In contrast, at 15-m, all particles loop into the eddy, with a radius consistent with the SVPs trajectories. Simulations initialized on May 8 and May 9 exhibit a

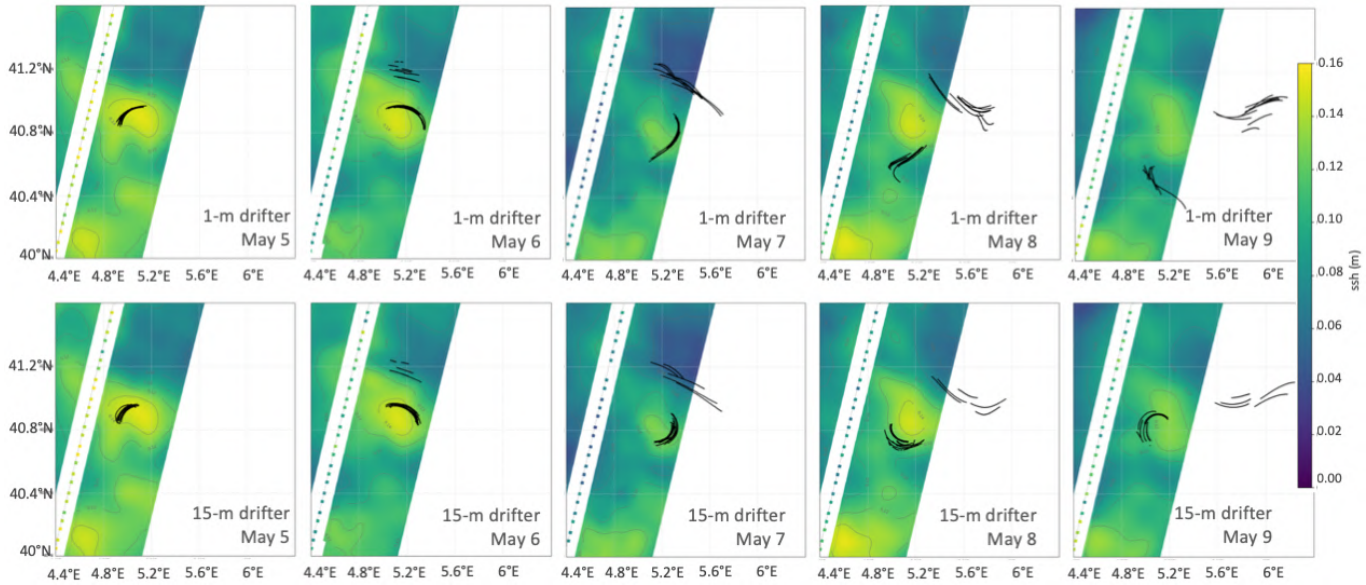

Figure 10. Evolution of 1-m (top) and 15-m (down) drifter trajectories from May 5 to 9 on the SWOT ssh (m) of the day.

similar pattern: numerical particles initialized on 15-m drifters positions consistently remain within the eddy, while particles initialized on 1-m drifter trajectories are ejected from the anticyclone. These simulations suggest that SWOT data are in a better agreement with observations at the 15-m depth layer, which is less affected by small-scale air-sea interactions compared to the surface layer.

4 Discussion

4.1 Sea-surface height gradients as a driver of oceanic circulation

In this section, the potential physical drivers of *in-situ* drifter trajectories are further investigated. The analysis of daily SWOT ssh maps and drifter trajectories provides a complementary explanation for the different patterns observed in the trajectories of drifters at 1-m and 15-m depths. Fig.10 summarizes the progression of drifters between May 6 and May 10, highlighting two distinct factors. On May 7, the 15-m drifters begin to diverge from the 1-m drifters, following a smaller circular path. Consequently, their positions align with areas of higher ssh values (in yellow contour color) and their trajectories stay in the eddy's loop, while the 1-m drifters remain at the periphery of this patch, where ssh values are lower (in green contour color) and are ejected from the eddy. On May 8, a yellow patch of higher ssh appear southwest of the main anticyclonic structure: the 1-m drifters bypassed this region while 15-m SVPs continued their looping inside the eddy. This analysis tends to indicate that fine-scale ssh gradients strongly contribute to local surface dynamics and that SWOT is able to detect such features, confirming Barcelo *et al.*, 2021.

4.2 Influence of the wind forcing

The distinct trajectory characteristics observed at 1-m and at greater depths prompt an investigation into the effect of surface wind on these trajectories. Wind velocity fields from May 7 to May 9 are

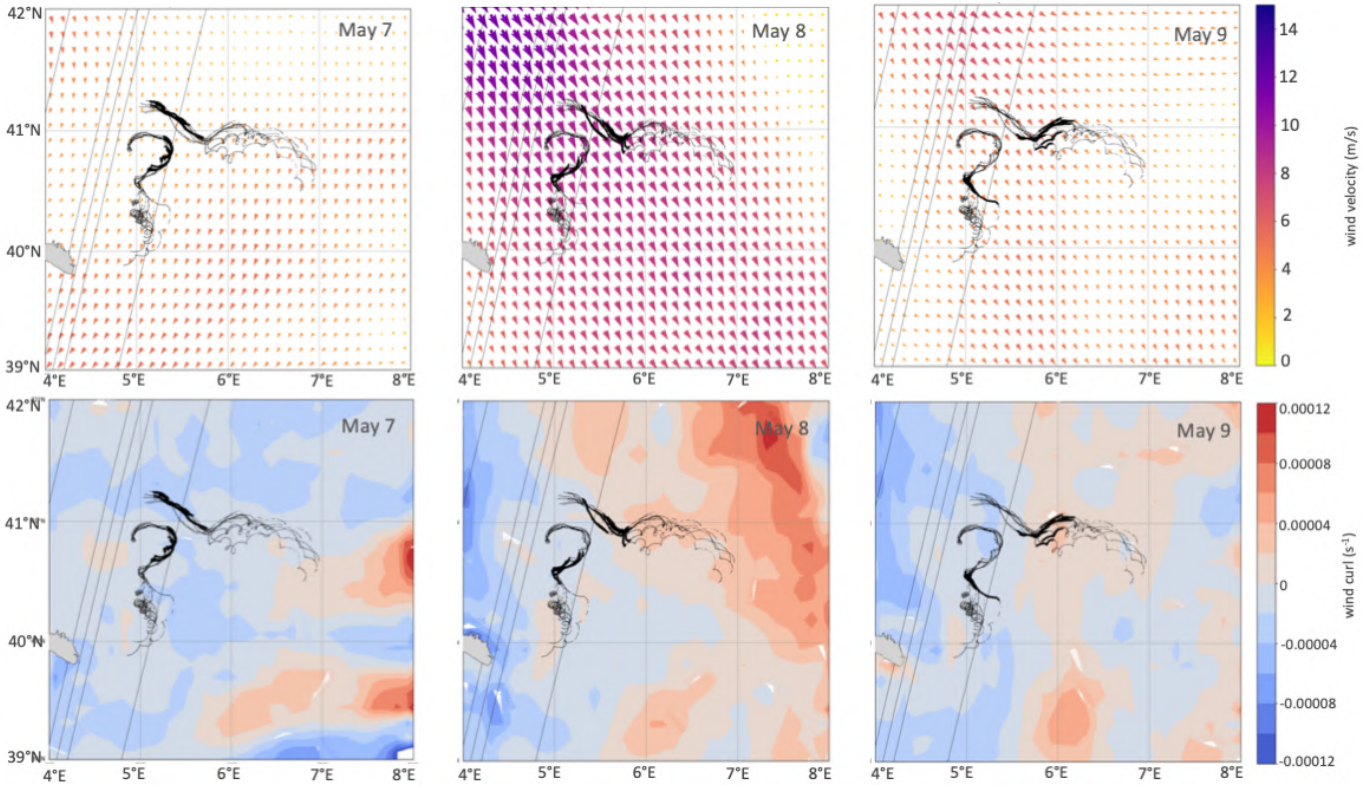

Figure 11. Wind velocities (m s^{-1}) (top) and vorticity (s^{-1}) (bottom) from May 7 to 9. 1-m drifters trajectories from May 5 to 12 are represented in black and superimposed in bold black for the same day as the wind. Source: CMEMS.

presented in Fig.11 (top). It is evident that an ephemeral yet intense Mistral episode occurred on May 8, coinciding with the period of shifting trajectories in both the anticyclone and the frontal feature. Three aspects of the wind on 1-m currents are investigated here: the mechanical friction on the water surface, the Ekman transport and its vorticity. First, mechanical friction over the water surface can lead to displacements of water masses. The wind on that day came from a N-W direction and, in the anticyclone, the trajectories shifted simultaneously according to direction of the wind, expelling the drifters from the solid-body rotation part of the eddy. The wind calmed down on May 9, and another strong Mistral episode occurred on May 10, explaining the formation of inertial oscillations. In the front, drifters were already moving south-eastward with the current flow before the wind event. At the end of the wind event (during the night of the 8 to the 9), they shifted in a different direction toward the north-west which cannot be explain directly by the wind friction. Second, Ekman transport leads to a drift of surface currents in the direction of the wind with a 45° deviation on the right in the northern hemisphere. After May 8, trajectories in the anticyclone point in a southern direction, and a strong inertial oscillation signal appears. Indeed, a 6-hour mean analysis of the wind event reveals that the most intense period of the wind event on the 8^{th} is between 12pm and 6pm, while the drifters are still on the anticyclone trajectories (as they shift only at the end of the day). Then, Ekman transport cannot conveniently match with the anticyclonic trajectories and their shift timing. Instead, in the front, drifters' trajectories are evolving in an opposite direction to what should be Ekman transport. As a consequence, it does not seem to be responsible for the drifter trajectory shift in the anticyclone or in the front. Another hypothesis can be deduced from

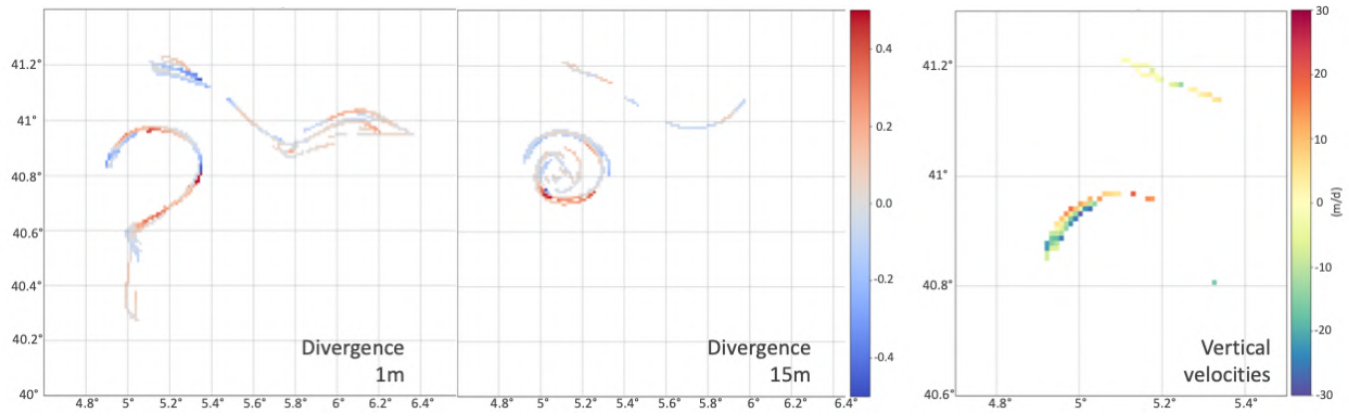

Figure 12. Lagrangian analysis of divergence at 1-m (left) and 15-m (middle) and vertical velocity w (m d^{-1}) (right) on filtered trajectories.

the third potential wind effect: Fig.11 (bottom) shows that before the 8, in the front, wind vorticity is mainly negative (anticyclonic) and shifted on that day to positive (cyclonic) in the area of the trajectory shift. An injection of wind vorticity in the frontal zone may explain the shift in vorticity of the current advecting the drifters.

4.3 Interactions between the anticyclonic and frontal features and influence on the divergence and vertical velocities signals

The presence of NIOs contributes significantly to the variability observed in the divergence and vertical velocity diagnostics, particularly within the anticyclonic feature (section 3.2). These oscillations induce swirling motions in the water masses, resulting in fluctuations in the measured signals over short time intervals. This leads to the mixed nature of the divergence (D) and vertical velocity (w) signals, characterized by an alternating pattern of positive and negative values, in coherence with trajectories affected by NIOs (Esposito *et al.*, 2023). By filtering the NIOs, the analysis gains a new perspective on the Lagrangian diagnostics. As depicted in Fig.12, after filtering, the divergence signals at both 1-m and 15-m depths show reduced intensity, with most of values between $\pm 0.4f$. Additionally, the signal becomes less mixed, displaying a clearer alternating pattern of positive and negative values. Even though the Butterworth filter effectively removes the dominant NIOs from the drifters' trajectories (see rotary spectra in Fig.7), a residual oscillating signal may still be present. These residual patterns could arise from interactions between the NIOs velocities and the larger-scale background velocity field, such as velocity shear.

The alternating pattern in divergence found at 1-m also leads to a similar pattern in w (right) with values oscillating between -28 to +20 m d^{-1}. The shift from negative to positive w values at a 1-m depth occurs gradually, with positive values appearing first on the external part of the trajectory, while the internal part remains mostly negative. These divergence and vertical velocity patterns are comparable to those observed during the CALYPSO campaign (Mahadevan, 2019), which took place in 2019 in the Alboran Sea: utilizing drifters deployed at 1 m and 15 m in anticyclonic eddies (more than 110 drifters deployed, see (Tarry *et al.*, 2021, 2022)), the Lagrangian analysis displayed a

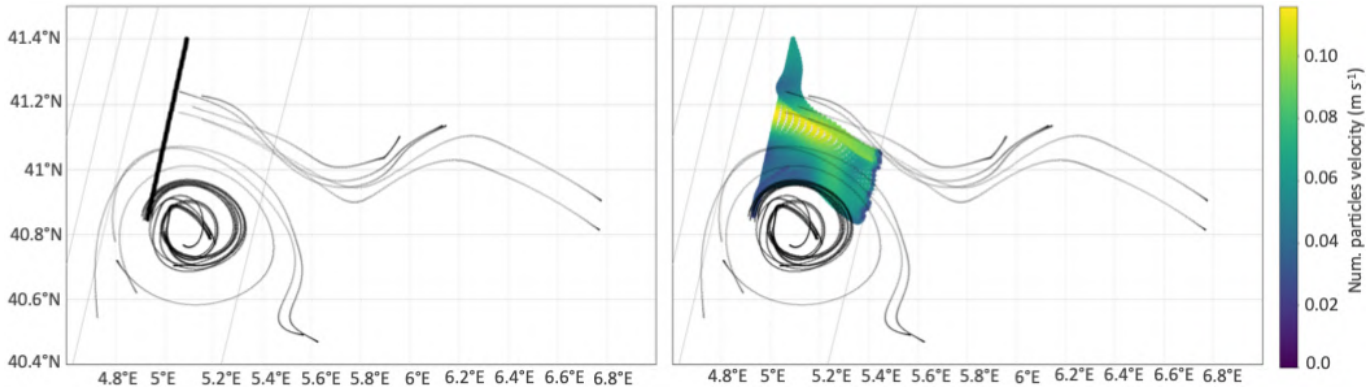

Figure 13. 3-days advection simulation made with the LAMTA toolbox and SWOT geostrophic velocities. The numerical particles were initialized on May 6 on an array crossing the eddy and the front (big black dots on the left) plotted on SWOT ssh (in m) of May 6 and were advection from May 6 to 8 (right). Colors represents the velocity of the numerical particles (in m s1). Filtered SVPs trajectories from BioSWOT-Med and C-SWOT from May 5 to 12 are represented in thin black lines.

similar alternation of positive and negative patterns along the filtered trajectories. Additionally, the same high variability and range of values for w, from -100 to +45 m d^{-1}, were observed, consistent with those found during BioSWOT-Med ($\pm$80 m d^{-1}). Combined density measurements made by a CTD during CALYPSO explained the alternating pattern as a more complex secondary ageostrophic vertical circulation in a zone of subduction of water masses (as described by McWilliams, 2016). It is possible that a secondary circulation is also responsible for the pattern observed during BioSWOT-Med, but the lack of available density profiles in depth for this space and time window does not make possible to draw the same conclusion yet. Modelling studies should also provide valuable insights.

Other sub-mesoscale hypotheses may also explain this specific ocean dynamics. It is possible that the low-pass filter removed other small space-time scale phenomena important for understanding local ocean dynamics. An agitated sea state could give rise to waves and rolls impacting the divergence signal and compatible with the space and time resolution of the signal but cruise logbook reports a calm sea state, confirmed by wind satellite observations. Langmuir circulation, associated with specific moderate wind conditions, could also have a compatible space-time scale but no complementary data are available to support this hypothesis at this stage.

A closer look at the trajectories of the ARGO floats and the C-SWOT SVPs drifters (Fig.4, bottom) provides further insights: they described a larger loop than the BioSWOT-Med SVPs and it took them approximately seven days to complete a full loop around the eddy (compared to less than four days for the BioSWOT-Med SVPs). According to the Rankine model, they must have been located outside the solid-body rotation of the anticyclone (where the angular velocity is constant and the tangential velocity increases with distance from the eddy center), in the potential eddy where the rotational velocity decreases inversely with distance from the eddy center. The question remains whether the BioSWOT-Med 1-m drifters were located inside the solid-body rotation or just outside it. If they were at the edge of the anticyclone (which would be a sort of "frontal" area of the an-

ticyclone), it may support the hypothesis of secondary circulation. To further appreciate the ocean dynamics between the two features and their possible interactions, an another LAMTA simulation was run with 60 numerical particles initialized on an array that goes from the location of deployment of the drifters in the anticyclone to the front (see black dots on Fig.13, left). The simulation was run on three days from May 6 to 8 (middle) and shows that the drifters in the front were deployed just at the southern edge of the front were the velocities of the numerical particles are the highest (in yellow), over 0.2 m s^{-1}. At the beginning of the advection, velocities in the eddy are the lowest, around 0.02 m s^{-1} (in blue) and a strong contrast exist between the front and the anticyclone. As the particles are moving eastward, the velocities of the particles close to the eddy center are increasing to 0.08 m s^{-1} (in green) and the zone between the anticyclone and the front becomes rather homogeneous in terms of velocities which could suggest that some interaction between the two features is happening. The numerical particles rapidly leave the SWOT swaths which prevents a more detailed analysis at this stage.

Nevertheless, what this analysis suggests is that interactions may exist between the two fine-scale structures, the front and the anticyclone, coexisting in a small geographic area. The visualization of the trajectories on the chlorophyll-a map, a proxy for phytoplankton abundance, recorded by SENTINEL3 satellite on May 5 (Fig.14) provides additional information about the water masses in the studied area. Drifters in the front, at both 1-m and 15-m depths, appear to progress along an intermediate band at the boundary between two water masses with distinct chlorophyll-a concentrations (higher at the north and lower at the south). The 15-m drifters in the anticyclone looped within what seems to be a homogeneous water mass, while the 1-m drifters appear to have been ejected from the eddy into the southern surface water mass with an even lower chlorophyll-a concentration. The interactions detected on the LAMTA simulation could be responsible for this peculiar chlorophyll-a pattern. Coupled with the knowledge gained from this study on local ocean dynamics, it is possible to consider that the anticyclone drags part of the frontal water in its wake, creating the intermediate concentration patch in which the eddy loops, thereby affecting the chlorophyll a signal observed. Conversely, the frontal jet may influence the anticyclone's shape (elliptical versus circular) and its kinematic properties. Close interactions between such fine-scale structures have been little explored so far and merit further investigation.

5 Conclusion and perspectives

This analysis aimed to study the fine-scale ocean dynamics in the moderate-energy and oligotrophic Western Mediterranean Sea during the BioSWOT-Med campaign, utilizing complementary data from a limited set of 1-m and 15-m drifters strategically deployed which were enhanced by the high resolution of the newly launched SWOT satellite. This approach allowed to characterize a complex fine-scale oceanic landscape featuring an anticyclonic eddy and a frontal jet coexisting within a reduced area 30 km by 30 km. The Lagrangian analysis and the estimation of the kinematic properties of these two features revealed: i) the overall concordance of SWOT data with drifter data compared

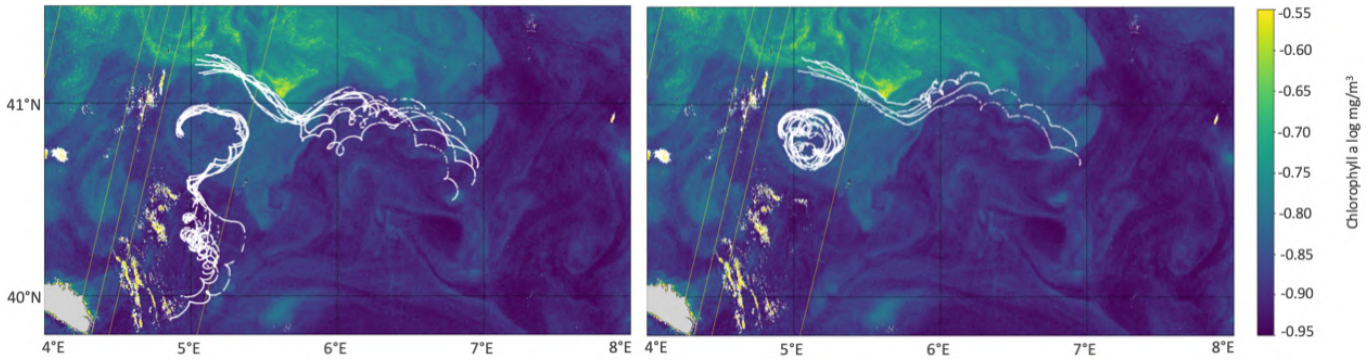

Figure 14. 1-m drifters trajectories (left) and 15-m drifter trajectories (right) (in white), from May 5 to 12, on the Chlorophyll-*a* concentration map (in log value, mg m^{-3}) of May 5. source: SENTINEL3 (CMEMS).

to the conventional satellite product DUACS, demonstrating SWOT's ability to identify fine-scale structures, ii) the influence of ssh and external wind forcing on the 1-m trajectories and some of the kinematic properties (vorticity in particular), iii) the peculiar patther of divergence and the vertical velocities and their dependency to small-scale processes (NIOs) and iv) the interactions between different fine-scale structures.

Part of these findings are consistent with other studies similarly conducted in the Western Mediterranean Sea and focused on frontal or anticyclonic structures (Balwada *et al.*, 2021; Esposito *et al.*, 2021; Tarry *et al.*, 2021, 2022); while others open new questions on fine-scale circulation and call for further investigation. The remaining alternating pattern observed in this study for the divergence and w signals after the filtering of NIOs is not fully explained by the drifter analysis alone. The hypothesis of a secondary circulation, which creates an ageostrophic vertical motion in frontal zones, would imply that the 1-m drifters had been deployed at the edge of the anticyclonic eddy in a "frontal" area of the eddy. Sub-mesoscale eddy structures overlaying, or interacting, with the mesoscale NBF are less documented than isolated fine-scale structures. Other instruments deployed during the BioSWOT-Med campaign, such as gliders, may add to the analysis: by providing density profiles across the two structures, they could shed a new light on the conditions of stratification of the water masses (at the end of May, the mixed layer may or may not be formed yet), on the structure of both features, on the localisation of the eddy's edge, etc. Without additional data, the question is left unresolved at this stage. Multiple other physical processes at different scales, such as near-internal waves created by the NIOs or Langmuir cells, could be responsible for the circulation pattern observed but would also require additional data to be confirmed. Particularly challenging to measure and critical to the understanding of biogeochemical processes, the vertical velocities obtained in the first 15 meters of the water column using the drifters will also have to be further compared to vertical velocities measured with other instruments deployed during the cruise: the free falling - Acoustic Doppler Current Profiler (FF-ADCP) (Comby *et al.*, 2022) and the Vertical Velocity profiler (Fuda *et al.*, 2023), see Doglioli & Gregory, 2023, for details. Additionally, a new version of the SWOT data is expected to be released next year, featuring interpolated ssh and geostrophic velocities outside the swaths. It will allow a deeper exploration of the dynamics between the two features, re-running

LAMTA simulations, which should allow for the investigation of the interactions between the anti-cyclonic eddy and the front in such close proximity.

The complexity of investigating and understanding the 3-D ocean fine-scale dynamics, because of the different physical processes at different space and time-scale, remains challenging until today. In this context, this analysis puts in perspective the synergies between *in-situ* measurements made with Lagrangian drifters and satellite remote-sensing, and advocates for the coupling of those to study fine-scale oceanic dynamics studies as well as with other complementary platforms and instruments. The results of this study, highlighting the great variability that characterizes the NBF region, set ground for their coupled study with biogeochemical processes to better understand vertical fluxes of nutrients and matter and their impact on the marine ecosystems productivity, which are other objectives of the BioSWOT-Med campaign. The many biogeochemical samplings that were made in or close to those features will benefit from the Lagrangian analysis. Preliminary results, obtained with the thermo-salinograph and automated flow cytometry measurements made during the cruise at the depth of 2 m, show that the eddy and the front presented contrasted physical characterises overlaying with a specific distribution of the phytoplankton communities, illustrating the "Paradox of the Plankton" (Hutchinson, 1961). A modelling approach enhanced by the newest SWOT resolution should be considered as well and would bring more insights in the comprehension of those mechanisms.

Bibliography

Balwada, Dhruv, Xiao, Qiyu, Smith, Shafer, Abernathey, Ryan, & Gray, Alison R. 2021. Vertical Fluxes Conditioned on Vorticity and Strain Reveal Submesoscale Ventilation. *Journal of Physical Oceanography*, **51**(9), 2883 – 2901. doi:10.1175/JPO-D-21-0016.1.

Barceló-Llull, Bàrbara, Pascual, Ananda, Sánchez-Román, Antonio, Cutolo, Eugenio, d'Ovidio, Francesco, Fifani, Gina, Ser-Giacomi, Enrico, Ruiz, Simón, Mason, Evan, Cyr, Fréderic, Doglioli, Andrea, Mourre, Baptiste, Allen, John T., Alou-Font, Eva, Casas, Benjamin, Díaz-Barroso, Lara, Dumas, Franck and, Gómez-Navarro Laura, & Muñoz, Cristian. 2021. Fine-Scale Ocean Currents Derived From in situ Observations in Anticipation of the Upcoming SWOT Altimetric Mission. *Front. Mar. Sci.*, 1070. doi:doi.org/10.3389/fmars.2021.679844.

Barral, Q-B., Zakardjian, B., Dumas, F., Garreau, P., Testor, P., & Beuvier, J. 2021. Characterization of fronts in the Western Mediterranean with a special focus on the North Balearic Front. *Progress In Oceanography*, **197**, 102636 (24p.). doi:10.1016/j.pocean.2021.102636.

Comby, C., Barrillon, S., Fuda, J.-L., Doglioli, A. M., Tzortzis, R., Grégori, G., Thyssen, M., & Petrenko, A. 2022. Measuring vertical velocities with ADCPs in low-energy ocean. *Journal of Atmospheric and Oceanic Technology*, **39**(11), 1669–1684. doi:10.1175/JTECH-D-21-0180.1.

Davis, Russ, E. 1985. Drifter observations of coastal surface currents during CODE: The method and descriptive view. *J. Geophys. Res.*, **90(C3)**(10), 4741– 4755. 10.1029/JC090iC03p04741.

Della Penna, Alice, De Monte, Silvia, Kestenare, Elodie, Guinet, Christophe, & d'Ovidio, Francesco. 2015. Quasi-planktonic behavior of foraging top marine predators. *Scientific Reports*, **5**(18063). doi:10.1038/srep18063.

Dickey, Tommy, & Bidigare, Robert. 2005. Interdisciplinary oceanographic observations: The wave of the future. *Scientia Marina*, **69**, 23–42. doi:10.1016/S0924-7963(03)00011-3.

Doglioli, A.M., & Gregory, G. 2023. *BioSWOT-Med cruise, RV L'Atalante.* doi:10.17600/18002392.

Doglioli, A.M., Grégori, G., D'Ovidio, F., Bosse, A., Pulido E., Carlotti, F., Lescot, M., Barani, A., Barrillon, S., Berline, L., Berta, M., Bouruet-Aubertot-P., Chirurgien, L., Comby, C., Cornet, V., Cotté, C., Della Penna, A., Didry, M., Duhamel-S., Fuda, J.-L., Gastauer, S., Guilloux, L., Lefèvre, D., Le Merle, E., Martin, A., Mc Cann, D., Menna, M., Nunige, S., Oms, L., Pacciaroni, M., Petrenko, A., Rolland, A., Rousselet, L., & Waggonet, E.M. 2024. *BioSWOT Med. Biological applicati.ons of the satellite Surface Water and Ocean Topography in the Mediterranean. Ref. Rapport de campagne. Université Aix-Marseille.* doi:10.13155/100060.

d'Ovidio, Francesco, Della Penna, Alice, Trull, Thomas W, Nencioli, Francesco, Pujol, M-I, Rio, M-H, Park, Y-H, Cotté, Cédric, Zhou, Meng, & Blain, Stéphane. 2015. The biogeochemical structuring role of horizontal stirring: Lagrangian perspectives on iron delivery downstream of the Kerguelen Plateau. *Biogeosciences*, **12**(19), 5567–5581. doi:10.5194/bg-12-5567-2015.

d'Ovidio, Francesco, Pascual, Ananda, Wang, Jinbo, Doglioli, Andrea, Jing, Zhao, Moreau, Sebastien, Grégori, Gérald, Swart, Sebastiaan, Speich, Sabrina, Cyr, Frederic, *et al.* 2019. Frontiers in Fine-Scale in situ Studies: Opportunities During the SWOT Fast Sampling Phase. *Front. Mar. Sci.*, **6**, 168. doi:10.3389/fmars.2019.00168.

Esposito, Giovanni, Berta, Maristella, Centurioni, Luca, Johnston, T.M. Shaun, Lodise, John, Özgökmen, Tamay, Poulain, Pierre-Marie, & Griffa, Annalisa. 2021. Submesoscale Vorticity and Divergence in the Alboran Sea: Scale and Depth Dependence. *Frontiers in Marine Science*, **8**. doi:10.3389/fmars.2021.678304.

Esposito, Giovanni, Donnet, Sebastien, Berta, Maristella, Shcherbina, Andrey Y., Freilich, Mara, Centurioni, Luca, D'Asaro, Eric A., Farrar, J. Thomas, Johnston, T. M. Shaun, Mahadevan, Amala, Özgökmen, Tamay, Pascual, Ananda, Poulain, Pierre-Marie, Ruiz, Simón, Tarry, Daniel R., & Griffa, Annalisa. 2023. Inertial Oscillations and Frontal Processes in an Alboran Sea Jet: Effects on Divergence and Vertical Transport. *Journal of Geophysical Research: Oceans*, **128**(3). doi:10.1029/2022JC019004.

Fuda, J.-L., Doglioli, A., Barrillon, S., Le Gal, P., Comby, C., & Petrenko, A. 2023. Estimating ocean vertical velocities using an autonomous multipurpose profiler. *In: IEEE International Workshop on Metrology for the Sea - Learning to Measure Sea Health Parameters (IEEE MetroSea)*. La Valetta, Malta: American Association for the Advancement of Science, for IEEE. doi:10.1109/MetroSea58055.2023.10317407.

Garreau, P. 2023. *C-SWOT-2023 cruise, RV Téthys II.* doi:10.17600/18002077.

Huntley, Helga S., Berta, Maristella, Esposito, Giovanni, Griffa, Annalisa, Mourre, Baptiste, & Centurioni, Luca. 2019. Conditions for Reliable Divergence Estimates from Drifter Triplets. *Journal of Atmospheric and Oceanic Technology*, **39**(10), 1499 – 1523. doi:10.1175/JTECH-D-21-0161.1.

Hutchinson, G., E. 1961. The Paradox of the Plankton. *The American Naturalist*, **95(882)**, 137–145. www.jstor.org/stable/2458386.

Mahadevan, A. 2019. *CALYPSO cruise, RV Pourquoi pas ?* doi:10.17600/18001177.

Mahadevan, Amala. 2016. The impact of submesoscale physics on primary productivity of plankton. *Annu. Rev. Mar. Sci.*, **8**, 161–184. doi:10.1146/annurev-marine-010814-015912.

McGillicuddy, Dennis, J. 2016. Mechanisms of Physical-Biological-Biogeochemical Interaction at the Oceanic Mesoscale. *Annu. Rev. Mar. Sci.*, **8**, 125–159. doi:10.1146/annurev-marine-010814-015606.

McWilliams, J.C. 2016. Submesoscale currents in the ocean. *Proc. R. Soc. A*. doi:10.1098/rspa.2016.0117.

Molinari, R., & Kirwan, A. D. Jr. 1975. Calculation on Differential Kinematic Properties from Lagrangian Observations in the Western Carribean Sea. *Jornal of Physical Oceanography*, **5**.

Moutin, T., Doglioli, A. M., de Verneil, A., & Bonnet, S. 2017. Preface: The Oligotrophy to the UlTra-oligotrophy PACific Experiment (OUTPACE cruise, 18 February to 3 April 2015). *Biogeosciences*, **14**(13), 3207–3220. doi:10.5194/bg-14-3207-2017.

Niiler, Pearn P, Sybrandy, Andrew S., Bi, Kenong, Poulain, Pierre M., & Bitterman, David. 1995. Measurements of the water-following capability of holey-sock and TRISTAR drifters. *Deep Sea Research I*, **42**(11112). doi:.

Novelli, Guillaume, Guigand, Cédric, M., Cousin, Charles, Ryan, Edward, H., Laxague, Nathan, J. M., Dai, Hanjing, Haus, Brian, K., & Özgökmen, Tamay, M. 2017. A Biodegradable Surface Drifter for Ocean Sampling on a Massive Scale. *J. Atmos. Oceanic Technol.*, **34**. doi:10.1175/JTECH-D-17-0055.1.

Petrenko, A., Doglioli, A., Nencioli, F., Kersalé, M., Hu, Z., & d'Ovidio, F. 2017. A review of the LATEX project: mesoscale to submesoscale processes in a coastal environment. *Ocean Dynam.*, **67**(3-4), 513–533. doi:10.1007/s10236-017-1040-9.

Rousselet, L., d'Ovidio, F., Izard, L., Della Penne, A., Petrenko, A., Barrillon, S., Nencioli, F., & Doglioli, A. submitted. A Software Package for an Adaptive Satellite-based Sampling for Oceanographic cruises (SPASSOv2.0): tracking fine scale features for physical and biogeochemical studies. *(submitted, JTECH-D-240071)*.

Saucier, J.W. 1953. Horizontal deformation in atmospheric motion. *American Geophysical Union*, **34**(5), 709–719.

Tarry, D. R., Essink, S., Pascual, A., Ruiz, Poulain, P.M., Özgökmen, T., Centurioni, L. R., , Farar, T.J., Shcherbina, A., T., Mahadevan, A., & d'Asaro, E. 2021. Frontal convergence and vertical velocity measured by drifters in the Alboran Sea. *Journal of Geophysical Research*, **49**. doi:10.1029/2020JC016614.

Tarry, D. R., Ruiz, S., Johnston, T. M. S., Poulain, P.M., Özgökmen, T., Centurioni, L. R., Berta, M., Esposito, G., Farar, T.J., T., Mahadevan, A., & Pascual, A. 2022. Drifter observations reveal intense vertical velocity in a surface ocean front. *Geophysical Research Letters*, **49**. doi:10.1029/2022GL098969.

Thomas, Leif, N., Tandon, Amit, & Mahadevan, Amala. 2008. Submesoscale processes and dynamics. *Washington DC American Geophysical Union Geophysical Monograph Series 177*, 17–38. doi:10.1029/177GM04.

Troupin, C., Pascual, A., Ruiz, S., Olita, A., Casas, B., Margirier, F., Poulain, P.-M., Notarstefano, G., Torner, M., Fernández, J. G., Rújula, M. À., Muñoz, C., Alou, E., Ruiz, I., Tovar-Sánchez, A., Allen, J. T., Mahadevan, A., & Tintoré, J. 2019. The AlborEX dataset: sampling of sub-mesoscale features in the Alboran Sea. *Earth System Science Data*, **11**, 129– 145. doi:10.5194/essd-11-129-2019.

Tzortzis, Roxane, Doglioli, Andrea M, Barrillon, Stéphanie, Petrenko, Anne A, d'Ovidio, Francesco, Izard, Lloyd, Thyssen, Melilotus, Pascual, Ananda, Barceló-Llull, Bàrbara, Cyr, Frédéric, Tedetti, Marc, Bhairy, Nagib, Garreau, Pierre, Dumas, Franck, & Gregori, Gérald. 2021. Impact of moderately energetic fine-scale dynamics on the phytoplankton community structure in the western Mediterranean Sea. *Biogeosciences*, **18**(24), 6455–6477. doi:10.5194/bg-18-6455-2021.

Abstract

The fine-scale oceanic circulation, composed of eddies, fronts, and filaments, is highly variable in time and space. Associated with 3-D velocity fields, they are crucial for biogeochemical processes involving vertical exchanges, especially in oligotrophic moderate-energy environments like the Mediterranean Sea, but yet under-sampled due to the complexity of *in-situ* measurements. To address this gap, and coinciding with the launch of the new Surface Water and Ocean Topography (SWOT) satellite, the BioSWOT-Med campaign was organized in April 2023 to sample the North Balearic Front using, among other instruments, 1-m and 15-m depth drifters. SWOT enabled the targeting of an anticyclonic eddy and a frontal jet. Lagrangian diagnostics revealed the significant roles of wind and sea-surface height in driving local surface circulation and showed an alternating pattern of vertical velocities within the anticyclone, likely explained by a secondary vertical ageostrophic circulation. This raises questions about the interactions between these features and their impact on local ocean dynamics, highlighting the complexity of fine-scale circulation in the region. Coupling this analysis with biogeochemical results from the campaign and numerical modeling studies should allow for a more precise reconstruction of the area's circulation and a deeper understanding of the link between the physical characteristics of water masses and their impact on the oceanic environment.

Resumé

La circulation océanique à fine échelle, composée de tourbillons, de fronts et de filaments, est très variable dans le temps et l'espace. Associées à des champs de vitesse 3-D, ces structures impactent fortement les processus biogéochimiques impliquant des échanges verticaux, notamment dans les environnements oligotrophes à énergie modérée comme en Mer Méditerranée. Elles sont toutefois sous-échantillonnées en raison de la complexité de mise en oeuvre des mesures *in-situ*. Coïncidant avec le lancement du nouveau satellite Surface Water and Ocean Topography (SWOT), la campagne BioSWOT-Med a été organisée en avril 2023 pour échantillonner la dynamique du Front Nord-Baléares à l'aide, entre autres, de bouées dérivantes à 1 m et 15 m de profondeur. SWOT a permis de cibler un tourbillon anticyclonique et un jet frontal. Les diagnostics lagrangiens ont révélé les rôles significatifs du vent et de la hauteur de la surface libre. Ils ont également montré un motif alterné de vitesses verticales dans l'anticyclone, possiblement expliqué par la présence d'une circulation verticale secondaire âgeostrophique. Le couplage avec les résultats biogéochimiques de la campagne et une étude de modélisation numérique plus approfondie devrait permettre une reconstruction précise de la circulation et une compréhension approfondie du lien entre les caractéristiques physiques des masses d'eau et leur impact sur l'environnement océanique.